ONE-DIMENSIONAL MODEL OF THE MOTION OF A CONCENTRATED DISPERSE MIXTURE IN AN ANNULAR DUCT

D. V. Bakonin, V. A. Drach, and E. M. Dyn'kin

UDC 678.7:66.011

The one-dimensional motion of a concentrated disperse mixture consisting of large granules of polyethylene (the disperse phase) and water (the carrier phase, i.e., the dispersion medium) in an annular duct is investigated. The duct is bounded on the outside by the impermeable wall of a cylinder of radius R_2, and on the inside by a cylindrical grid of radius R_1; both boundaries are vertically oriented. A mixer is placed inside the cylindrical grid, its axis aligned with the axis of the cylinders. This type of problem of the motion of a mixture arises in the investigation of the polymerization initiation process in the production of synthetic rubbers. In this process, active polymerization centers are formed in the mixing of monomers, a solvent, and coarse granules of an alkali metal [1]. The specific features of the real mixture are investigated in the model medium of water containing polyethylene granules.

Experimental

The experimental apparatus consisted of three identical sections (Fig. 1). The cylindrical casing 1 was made of clear plastic. The apparatus was sectioned by means of the separator disks 2, in which the windows 3 were made. The cylindrical metal grids 4 were installed coaxially in each section. The mixer 5 had a trapezoidal four-paddle configuration with projecting flanges along the edges. The reflecting disks 6 were mounted on the grid at the level of the flanges.

Experiments to measure the circumferential velocity v_1 of the carrier phase were performed on an apparatus with $R_2 = 0.125$ m. The height of each section was 0.265 m. The grid radius R_1 was varied from 0.06 to 0.089 m, and the mixer radius from 0.049 to 0.073 m, respectively. Square-mesh grids with mesh areas of 0.025, 1, and 4 mm^2 were used in the experiment. The angular velocity ω of the mixer was varied from 30 to 145 sec^{-1}, and the relative volume content α_2 of the granules from 0.05 to 0.22. The cylindrical polyethylene granules (density 950 kg/m^3) had a diameter of 5 mm and a length of 6 mm.

The experiments showed that the motion of the mixture takes place mainly along arcs of a circle. The measurements of v_1 were carried out with a Pitot tube in the middle cross section. The tube had two channels of diameter 1 mm, which were mutually oriented at 90° and were designed to measure the static and dynamic pressure of the flow. The tube was set up in a horizontal plane. Figure 2 shows the measured values of v_1 for $R_1 = 0.06$ m, a 1 × 1 mm grid mesh, $\alpha_2 = 0.125$, and ω = 40, 64, 93, 115, and 145 sec^{-1} (open circles 1-5, respectively). Also shown are the values of v_1 in the absence of the granules ($\alpha_2 = 0$) for ω = 40, 64, 93, 115, and 145 sec^{-1} (dark circles 1-5).

Figure 3 shows the measured values of v_1 for $R_1 = 0.075$ m, a 1 × 1 mm grid mesh, ω = 93 sec^{-1} and α_2 = 0, 0.045, 0.125, 0.16, and 0.22 (points 1-5).

The following characteristic features are discerned in the flow of a mixture with a sufficiently high content of granules: 1) The carrier phase is abruptly retarded at the grid, its deceleration increasing with the value of α_2; 2) for a sufficient distance between the grid and the wall, a pronounced minimum of the v_1 profile is observed at a distance of the order of three granule diameters from the grid; 3) after the minimum, the v_1 profile has a maximum, and then the velocity drops slightly or stabilizes. For a small granule content ($\alpha_2 \le 0.05$) the v_1 profile is similar to the profile of Couette flow (between rotating cylinders).

The measurements of v_1 were carried out until uniform mixing of the granules throughout the volume could no longer be maintained. At $\alpha_2 > 0.22$ the visible mobility of the granules began to decreases, and clusters of granules with a low mobility relative to one another were

---

Leningrad. Translated from Zhurnal Prikladnoi Mekhaniki i Tekhnicheskoi Fiziki, No. 4, pp. 77-83, July-August, 1985. Original article submitted May 15, 1984.

0021-8944/85/2604-0519$09.50

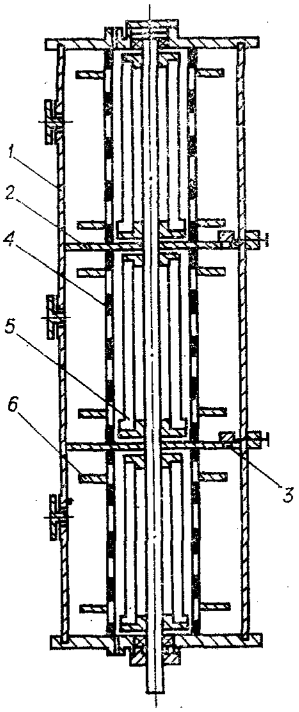

Fig. 1

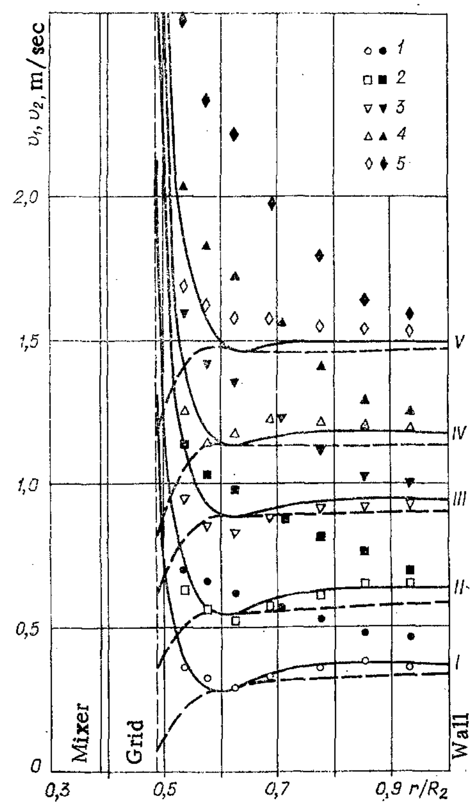

Fig. 2

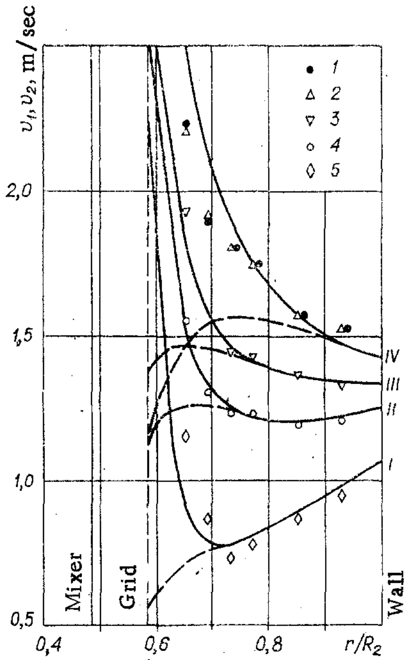

Fig. 3

formed at isolated locations. These clusters continued to move slowly in a circle at first, but this motion ceased at $\alpha_2 \sim 0.26$.

The power spent in stirring the mixture was determined by measuring the difference in the power consumed by the electric motor driving the mixer in the filled apparatus and in the no-load regime, i.e., in the absence of the mixture.

We now formulate a one-dimensional model of the steady flow of the mixture on the basis of concepts developed previously [2-4]. This model adequately describes the experimental data and makes it possible to explain the specific features of the flow of the mixture.

One-Dimensional Model of the Motion of the Mixture

We regard the disperse phase as a pseudogas of granules (spheres of radius a) [2, 3]. The pseudogas creates a mean pressure p_2 and has a mean effective pseudoviscosity μ_2. Each granule participates in the mean motion with a velocity v_2 and in the random (fluctuation) motion with a velocity $w_2(\nu)$, where ν indexes the granules. The mean values of the random velocities are assumed to be equal to zero. In the ensuing discussion we use the mean-square velocity $w_{2*}^2 = \frac{1}{N}\sum_{\nu=1}^{N} |\mathbf{w}_2|^2(\nu)$, where N is the number of granules. The materials of the phase have nearly equal densities.

A granule is acted upon by the mean forces of viscous friction f_μ and of the additional masses f_M, the Magnus force f_m, and the buoyancy (Archimdes force) f_A.

Velocities of the Phases. Let v_{ir}, $v_{i\theta}$, v_{iz} denote the components of the vectors v_i ($i = 1, 2$) along the axes of a cylindrical coordinate system r, θ, z. We assume that the motion of the mixture takes place along circles with centers on the z axis, so that

$$v_{ir} = v_{iz} = 0,\ v_{i\theta} = v_{i\theta}(r) = v_i\,, \quad v_1 > v_2.$$

Then the mean force f_μ has a nonzero projection only on the θ axis (f_μ), f_m and f_M only on the r axis (f_m), and f_A only on the r(f_A) and z axes.

We first consider the model of the initial approximation. We assume that the mean viscous friction force $f^{12}{}_\mu$ in interaction of the phases is determined mainly by the effective viscosity μ_1 of the carrier phase and the relative slip velocity $v_{12} = v^0{}_1 - v^0{}_2$, where $v^0{}_1$ and $v^0{}_2$ are the velocities of the initial approximation. Then in the initial approximation

$$f_\mu^{12} = -f_\mu^{21} = K\mu_1 v_{12}, \tag{1}$$

where K is a parameter depending on a, w_{2*}, and $\rho^0{}_1$ ($\rho^0{}_1$ is the density of the material of the carrier phase).

The equations of motion of the disperse mixture have the form

$$Lv_1^0 \equiv \frac{d^2 v_1^0}{dr^2} + \frac{1}{r}\frac{dv_1^0}{dr} - \frac{v_1^0}{r^2} = k_1(v_1^0 - v_2^0); \tag{2}$$

$$Lv_2^0 \equiv \frac{d^2 v_2^0}{dr^2} + \frac{1}{r}\frac{dv_2^0}{dr} - \frac{v_2^0}{r^2} = k_2(v_2^0 - v_1^0), \tag{3}$$

where $k_1 = nK$; $k_2 = (\mu_1/\mu_2)k_1$; $n = 3\alpha_2/4\pi a^3$ is the granule concentration.

For the new variables $f_1(r\sqrt{k_1 + k_2}) = v^0{}_1 - v^0{}_2$, $f_2(r) = v^0{}_1 + (k_1/k_2)v^0{}_2$, Eqs. (2) and (3) are reduced to modified Bessel equations:

$$Lf_1 = f_1; \tag{4}$$

$$Lf_2 = 0. \tag{5}$$

In accordance with the experimental data, we use the decreasing solutions of (4), (5), which are modified Bessel functions $K_1(r)$. Setting $r\sqrt{k_1 + k_2} \geq 2$ and restricting the asymptotic expansion of $K_1(r)$ the first term, we obtain

$$v_1^0 = Ar + Br^{-1} + r^{-\frac{1}{2}}C_1 \exp(-r\sqrt{k_1 + k_2}); \tag{6}$$

$$v_2^0 = Ar + Br^{-1} - \frac{\mu_1}{\mu_2}C_1 r^{-\frac{1}{2}}\exp(-r\sqrt{k_1 + k_2}), \tag{7}$$

where A, B, and C_1 are constants.

The velocity $v^0{}_1$ is the sum of two functions: a) a function analogous to the Couette velocity profile ($Ar + Br^{-1}$), which establishes the general velocity level; b) an exponential function that decreases rapidly near the grid: $C_1 r^{-1/2}\exp(-r\sqrt{k_1 + k_2})$.

The velocity $v^0{}_1$ decreases, and $v^0{}_2$ increases in the direction toward the wall. This model describes the abrupt slowing of v_1 at the grid, which was observed experimentally. The effect is attributed to a certain increase in the granule concentration at the grid and a change in the flow conditions around them in comparison with the main volume. The function b) only slightly affects the nature of the $v^0{}_1$ profile at the wall, where the latter is determined mainly by the function a), which decreases monotonically from the grid to the wall. The constants A, B, and C_1 are evaluated according to the experimental data. Then the velocity $v^0{}_2$ is completely determined by the specification of the ratio $k_2/k_1 = \mu_1/\mu_2$, where $v^0{}_2 < v^0{}_1$.

The model (6), (7) describes only monotonic variations of the velocities v_1 and v_2. Such profiles of v_1 are typical of not too concentrated mixtures ($\alpha_2 < 0.1$) or when the ratio of the channel width to the granule diameter $(R_2 - R_1)/2a < 6$. However, the proposed mechanism does not account for the observed acceleration of the carrier phase after the abrupt deceleration zone. To describe this effect we introduce additional assumptions.

The model (6),(7) incorporates a linear dependence of the friction force f_μ on the velocities v_1 and v_2. The true expression for f_μ, of course, is nonlinear, and so the true profiles of the velocities v_1 and v_2 differ from the velocities $v^0{}_1$ and $v^0{}_2$ given by the model (6), (7). A comparison of the calculated and experimental values of v_1 shows, however, that these deviations are not too great. We can therefore assume that $v_1 = v^0{}_1 + \Delta v_1$, $v_2 = v^0{}_2 + \Delta v_2$, where Δv_1 and Δv_2 are small corrections. On the other hand, the relative variations of the experimental values of v_1 along the radius is also small, and it is a reasonable assumption to "freeze" the coefficients in the linear terms of the expansion in powers of Δv_1 and Δv_2.

The resulting first-approximation system has the form

$$L\Delta v_1 = k_3\Delta v_1 - k_4\Delta v_2; \tag{8}$$

$$L\Delta v_2 = -k_5\Delta v_1 + k_6\Delta v_2. \tag{9}$$

It is natural to assume that the difference between Eqs. (8) and (9) in this approximation is elicited, as in the case of (6) and (7), only by the difference in the effective viscosities μ_1 and μ_2, i.e.,

$$k_3/k_6 = k_4/k_5 = k_1/k_2 = \mu_2/\mu_1 > 1. \tag{10}$$

For any values of the coefficients k_3, k_4, k_5, and k_6 the solutions of the system (8), (9) are represented by linear combinations of first-order modified Bessel functions of the form $F(r\sqrt{\lambda})$, where λ is one of the two eigenvalues of the matrix of coefficients. For $\lambda < 0$ such a function oscillates, in contradiction with the experimental, and such solutions must be rejected. Solutions that grow in the radial direction (functions of the second kind) must be similarly rejected on the basis of physical considerations.

For small values of λ the corresponding components of the solution differ very little from the component of the Couette profile B/r and cannot be distinguished from the initial approximation $v^0{}_1$, $v^0{}_2$. Finally, inasmuch as $v^0{}_1$ and $v^0{}_2$ practically coincide at a certain distance from the grid, in which case it is logical to expect the velocity v_2 of the granules not to exceed the velocity v_1, we obtain the necessary condition $\Delta v_2 < \Delta v_1$.

An analysis of the resulting constraints on the coefficients k_3 and k_4 leads to the conclusion that the system (8), (9) in the first approximation has the form

$$L\Delta v_1 = k_3\Delta v_1; \tag{11}$$

$$L\Delta v_2 = \frac{\mu_1}{\mu_2} k_3\Delta v_2. \tag{12}$$

As before, we take the functions $K_1(r)$ as the solutions of Eqs. (11) and (12). Assuming that $r\sqrt{\frac{\mu_1}{\mu_2}k_3} \geqslant 2$ and restricting the asymptotic expansion of $K_1(r)$ to the first term, we obtain

$$v_1 = Ar + Br^{-1} + r^{-1/2}(C_1 \exp(-r\sqrt{k_1 + k_2}) + C_2 \exp(-r\sqrt{k_3})); \tag{13}$$

$$v_2 = Ar + Br^{-1} + r^{-1/2}\left(-\frac{\mu_1}{\mu_2} C_1 \exp(-r\sqrt{k_1 + k_2}) + C_3 \exp\left(-r\sqrt{\frac{\mu_1}{\mu_2}k_3}\right)\right), \tag{14}$$

where C_2 and C_3 are constants, $C_2 < 0$.

In this case the velocity v_1 is the sum of three functions, two of which are described above, while the third, $C_2 r^{-1/2} \exp(-r\sqrt{k_3})$, is a growing exponential function, which provides the pronounced minimum of the v_1 profile for a sufficient radial width of the duct. The sum of these functions describes the above-indicated features of the v_1 profile. The constants A, B, C_1, C_2, C_3, $k_1 + k_2$, and k_3 are evaluated according to the experimental data.

Viscosity of the Carrier Phase and Distribution of Power Consumption in Stirring of the Mixture. To determine μ_1 we use the experimental data on the determination of the power consumption N_0 in stirring of the mixture. We assume that this power is spent mainly in the dissipation of energy E_1 in the carrier phase and E_2 in the disperse phase, and also in overcoming the resistance of the granules in the flow around them (E_{12}), so that

$$N_0 = -E_1 - E_2 - E_{12}. \tag{15}$$

From the general expression for the dissipation of energy in a viscous fluid [5] we obtain (per unit height of the duct)

$$E_1 = -\pi\alpha_1\mu_1 \int_{R_1}^{R_2} \left(\frac{dv_1}{dr} - \frac{v_1}{r}\right)^2 r\,dr; \tag{16}$$

$$E_2 = -\pi\alpha_2\mu_1\frac{k_1}{k_2}\int\limits_{R_1}^{R_2}\left(\frac{dv_2}{dr}-\frac{v_2}{r}\right)^2 r\,dr; \tag{17}$$

$$E_{12} = -2\pi k_1\mu_1\int\limits_{R_1}^{R_2}(v_1-v_2)^2 r\,dr. \tag{18}$$

Then the value of μ_1 is uniquely determined from (15). The distribution of the power consumption is given by Eqs. (16)-(18).

Distribution of the Disperse Phase. It was assumed above that α_2 = const. To determine the distribution of the disperse phase along the duct (second approximation) we write $\alpha_2 = \alpha_2(r)$. We fix the profiles of the velocities v_1 and v_2 in this case.

The general equation of motion of the disperse phase in projection onto the r axis has the form

$$dp_2/dr = n(f_M + f_m + f_A). \tag{19}$$

For f_m and f_A we use the expressions [4]

$$f_A = \frac{4}{3}\pi a^3\rho_1^0\left(\frac{d_1v_1}{dt}-g\right); \tag{20}$$

$$f_m = \frac{2}{3}\pi a^3\rho_1^0\left(\frac{d_1v_1}{dt}-\frac{d_2v_2}{dt}\right), \tag{21}$$

in which $d_i/dt = \partial/\partial t + v^k{}_i(\partial/\partial x_h$.

Next we consider the expression for the Magnus force f_M. The cause of rotation of a granule is found mainly in the gradients of the mean velocities of the phases (if fluctuations and collisions of the granules are ignored). By analogy with [4], we set

$$\mathbf{f}_M = \frac{4}{3}\pi a^3\rho_1^0[(\mathbf{v}_1-\mathbf{v}_2)\times\nabla(\alpha_1\mathbf{v}_1+\alpha_2\mathbf{v}_2)]. \tag{22}$$

Using the previously established [2, 3] relation between p_2 and α_2, and taking expressions (20)-(22) into account, we obtain the following from (19):

$$\frac{d\alpha_2}{dr} = \frac{\alpha_2(1-1{,}16\alpha_2^{1/3})^2}{w_{2*}(1-0{,}773\alpha_2^{1/3})}\left[-(v_1-v_2)\frac{d}{dr}(\alpha_1v_1+\alpha_2v_2)-\frac{3}{2}\frac{v_1^2-v_2^2}{r}\right]. \tag{23}$$

We set w_{2*} = const.

A natural additional condition is given by specifying the mean content of the disperse phase:

$$\langle\alpha_2\rangle = \frac{\int\limits_{R_1}^{R_2} r\alpha_2(r)\,dr}{\int\limits_{R_1}^{R_2} r\,dr}. \tag{24}$$

Discussion of Results

It has been assumed in the calculations that the granules are spheres of diameter 2a with the same volume as the cylindrical granules used in the experiment.

Figure 2 shows the calculated values of v_1 (solid curves) and v_2 (dashed curves) for $\alpha_2 = 0.125$ and ω = 40, 64, 93, 115, and 145 $\sec^{-1}$ (curves I-V, respectively). Figure 3 shows the same quantities as in Fig. 2 for $\omega = 93$ $\sec^{-1}$ and α_2 = 0.22, 0.16, 0.125, and 0.045 (curves I-IV).

The experimental data were used to evaluate the constants in Eqs. (13) and (14). It was assumed that the v_1 profile at the wall is determined mainly by the constants A and B.

TABLE 1

No.	ω, sec^{-1}	μ_1, N·sec/m^2	N_0, W	$\frac{E_1}{N_0}\cdot 100\%$	$\frac{E_2}{N_0}\cdot 100\%$	$\frac{E_{12}}{N_0}\cdot 100\%$
1	30	0,25	6	32,8	0,8	66,4
2	40	0,45	15	33,0	0,7	66,3
3	64	0,94	58	33,4	0,6	66,0
4	93	1,27	137	33,6	0,6	65,8
5	115	1,76	265	33,6	0,7	65,7
6	145	2,45	544	33,7	0,7	65,6
7	159	3,53	909	33,5	0,7	65,8

TABLE 2

No.	α_2	μ_1, N·sec/m^2	N_0, W	$\frac{E_1}{N_0}\cdot 100\%$	$\frac{E_2}{N_0}\cdot 100\%$	$\frac{E_{12}}{N_0}\cdot 100\%$
1	0,045	4,25	280	48,6	0,3	51,1
2	0,062	4,11	280	47,8	0,5	51,7
3	0,087	3,87	274	45,8	1,1	53,1
4	0,125	3,71	272	42,4	1,9	55,7
5	0,16	3,63	269	39,1	1,8	59,1
6	0,22	3,42	253	33,4	0,3	66,3

The dependence of these constants on ω was assumed to be linear, and their dependence on α_2 was assumed to be quadratic. Then the function $\psi(r) = \sqrt{r}(v_1 - Ar - Br^{-1})$ was plotted and exhibited abrupt variations at the grid. These results were used to find the constants C_1 and C_2, and it was assumed that they depend linearly on ω. The values of the constants $k_1 + k_2$ and k_3 were fixed for each ratio R_1/R_2 in the calculations. The tests with $\omega = 40$, 115 sec^{-1} were used to determine the indicated constants in Fig. 2, and the tests with $\alpha_2 =$ 0.045, 0.22 were used for Fig. 3. For the evaluation of the constant C_3 we assumed that the velocities v_1 and v_2 are equal at the wall (see Fig. 3) or at the minimum point (see Fig. 2).

The nature of the flow of the carrier phase is adequately described by the sum of the three functions indicated above. The calculated values of v_1 are finite at the grid. With an increase in ω (α_2 = const; see Fig. 2) the values of v_1 increase, but the nature of the v_1 profile is preserved. For each value of ω the velocity v_1 is a maximum at the grid, and then the v_1 profile acquires a pronounced minimum, after which v_1 varies only slightly.

With an increase in the granule content (ω = const; see Fig. 3) a significant deformation of the v_1 profile is observed. For $\alpha_2 \leq 0.045$ the granule content has scarcely any influence on v_1. With an increase in α_2 an ever-increasing retardation of the carrier phase is observed at the grid.

Table 1 gives the values of μ_1, N_0, E_1/N_0, E_2/N_0, and E_{12}/N_0 for various values of (1 × 1 mm grid mesh, $R_1 = 0.06$ m, $\alpha_2 = 0.125$). With an increase in the rpm of the mixer the values of μ_1 increase. A decrease in the radial dimensions of the channel causes μ_1 to increase (e.g., in the case $R_1 = 0.089$ m we have $\mu_1 = 30$ N·sec/m^2 at $\omega = 25$ sec^{-1} and $\mu_1 = 175$ N·sec/m^2 at $\omega = 145$ sec^{-1}). All of this is consistent with the known estimate for the turbulent viscosity [5].

The main power consumption (see Table 1) is spent in the fraction E_{12}. The least energy dissipation is in the disperse phase. With a decrease in the radial dimension of the channel, the power consumption increases and is redistributed, viz., the energy dissipation increases in the carrier and disperse phases, and the fraction E_{12} decreases. This is evidently related to enhancement of the influence of turbulent fluctuations, which results in an increase of w_{2*} and, as a consequence, smoothing of the v_1 profile.

Table 2 shows the same quantities as in Table 1 for various values of α_2 (1 × 1 mm grid mesh, $R_1 = 0.075$ m, $\omega = 93$ sec^{-1}). The decrease in the power consumption with increasing α_2 is associated with the decrease in the fraction E_1 and the increase in the fraction E_{12}. The first is caused by a decrease in the turbulence scale owing to a reduction in the mean free path of the granules, and also by the suppression of small-scale fluctuations as the granule concentration is increased. The increase in E_{12} is associated with the increase in α_2.

We now consider the distribution of the disperse phase in the channel. The solution of Eqs. (23) and (24) for various values of $\langle\alpha_2\rangle$ shows that α_2 remains practically constant at distances from the grid greater than two or three granule diameters. At smaller distances from the grid for a channel of sufficient radius $[(R_2 - R_1)/2a > 6]$ the solution predicts a decrease in α_2. However, the investigated model does not allow for processes near the grid, viz., the variation of the fluctuation velocities, inflow, and repulsion of the granules, etc. Consequently, the problem of the behavior of the granules near the grid requires additional investigation.

LITERATURE CITED

1. V. A. Drach, S. M. Krasil'nikov, G. M. Tolstopyatov, and M. L. Gol'din, "Mathematical description of the process of synthesis of general-purpose rubber," in: Abstracts of the Sixth All-Union Conference "Khimreaktor-6" [in Russian], Vol. 1, Dzerzhinsk (1977).
2. M. A. Gol'dshtik, "Theory of concentrated disperse systems," in: Proceedings of the International School on Transfer Processes in Fixed-Bed and Fluid-Bed Granular Materials [in Russian], Minsk (1977).
3. M. A. Gol'dshtik and B. N. Kozlov, "Elementary theory of concentrated systems," Zh. Prikl. Mekh. Tekh. Fiz., No. 4 (1973).
4. R. I. Nigmatulin, Fundamentals of the Mechanics of Heterogeneous Mixtures [in Russian], Nauka, Moscow (1978).
5. L. D. Landau and E. M. Lifshits, Continuum Mechanics [in Russian], GITTL, Moscow (1953); Fluid Mechanics, Pergamon, Oxford—New York (1959).

FORMATION OF FLOW IN A GASDYNAMIC MOLECULAR SOURCE AT LOW REYNOLDS NUMBERS

V. N. Gusev and A. I. Omelik

UDC 533.6.011.532.522.2

1. The usual means of creating a molecular beam in a gasdynamic source [1] is shown in Fig. 1. From the forechamber 1 the gas, with a pressure p_0 and a temperature T_0, expands through the nozzle 2 to a certain supersonic Mach number in the preskimmer chamber 3 ($0 \leq x \leq x_s$). In the process, a considerable part of the chaotic thermal motion of the molecules is converted into ordered mass motion. In the high-vacuum chamber 4 ($x > x_s$) a small part of this stream is subsequently formed into a molecular beam with the help of a conical intake — the skimmer 5; 6 is the boundary of the undisturbed region of the jet, 7 is a suspended shock, and 8 is the boundary of the jet.

For a Maxwell velocity distribution of the molecules with a superposed mass velocity v_m the intensity of such a source at the detection point x_d is [2]

$$I(x_d) = \rho(x_d)\, v_m x_d^2 = I(x_s)\left\{1 - \cos^2\psi\, e^{-S_s^2 \sin^2\psi}\, \frac{I_1(S_s \cos\psi)}{I_1(S_s)}\right\},$$

$$I_1(x) = \frac{1}{2} e^{-x^2} + \frac{x\sqrt{\pi}}{2}(1 + \operatorname{erf} x),$$

where ρ is the density; $S = (\sqrt{\kappa/2})M = v_m(2RT)^{-1/2}$ is the velocity ratio; κ is the ratio of specific heats; $\psi = \varphi + \gamma$. For small angles ψ, as is usually the case in such installations, the latter expression is simplified,

$$I(x_d) = I(x_s)\left[1 - e^{-\psi^2 S_s^2}\right] \tag{1.1}$$

Zhukovskii. Translated from Zhurnal Prikladnoi Mekhaniki i Tekhnicheskoi Fiziki, No. 4, pp. 83-91, July-August, 1985. Original article submitted April 16 1984.

0021-8944/85/2604-0525$09.50